

## Research Article

# Saturation Height Modelling for Tight Sandstone Reservoirs with Gas Diffusion Dynamics Taken into Account

Zhou Lyu <sup>1,2</sup>, Zhilun Yang,<sup>2</sup> Yuhong Hao,<sup>2</sup> Shunzhi Yang,<sup>2</sup> Liqiong Wang,<sup>3</sup> Sen Chang,<sup>2</sup> Xiaomin Xue,<sup>4</sup> and Jing Li<sup>5</sup>

<sup>1</sup>Gas Field Development Department, Research Institute of Petroleum Exploration & Development, PetroChina, Beijing 100083, China

<sup>2</sup>Sulige Development Branch, Changqing Oilfield Company, PetroChina, Wushen 017300, China

<sup>3</sup>Fourth Gas Production Plant, Changqing Oilfield Company, PetroChina, Wushen 017300, China

<sup>4</sup>Gas Field Development Division, Changqing Oilfield Company, PetroChina, Xi'an 710018, China

<sup>5</sup>Exploration Division, Changqing Oilfield Company, PetroChina, Xi'an 710018, China

Correspondence should be addressed to Zhou Lyu; lvzhou827@163.com

Received 6 December 2022; Revised 30 July 2023; Accepted 8 September 2023; Published 3 October 2023

Academic Editor: Azizollah Khormali

Copyright © 2023 Zhou Lyu et al. This is an open access article distributed under the Creative Commons Attribution License, which permits unrestricted use, distribution, and reproduction in any medium, provided the original work is properly cited.

Interpreting and predicting the saturation of tight sandstone gas reservoirs are the key task to improve the reservoir development. The role of gas diffusion dynamics is stronger than that of buoyancy during the gas accumulation of tight sandstone reservoirs. In this study, a saturation height model that takes gas diffusion dynamics into account is proposed, which can complement logging saturation interpretation and provide a better practice in saturation prediction. Taking the study of the Sulige tight sandstone gas reservoir in China as an example, the saturation height model compares the controlling factors and uncertainties affecting the saturation distribution, characterizes the complex gas-water distribution, and determines the lower gas charging limits. This study concludes that the configuration between gas diffusion dynamics and reservoir capillary pressure controls the distribution of saturation. The buoyancy effect only serves to improve the saturation at regional uplifts with good petrophysical properties. The different saturation characteristics in the central, western, and eastern parts of the Sulige gas field are precisely caused by the different configurations of source rock quality and reservoir quality. This study provides a key reference for static model and development deployment.

## 1. Introduction

The tight sandstone gas reservoirs (the gas flow permeability is expected to be less than 0.1 mD under reservoir conditions) are the rapid growth of unconventional gas reservoirs in China [1, 2]. In 2020, the tight gas production in China was beyond  $450 \times 10^8 \text{ m}^3$  per year [3], tens of times more than 20 years ago. With the deepening of exploration and development, tight sandstone gas reservoirs show complex gas-water distribution characteristics. Compared to conventional gas reservoirs, tight sandstone gas reservoirs generally do not have uniform gas-water contacts [4], and large-scale gas-water transition zones

generally appear [5], and even the phenomenon of water above the gas often appears. These geological features cause production problems in the development of tight gas reservoirs, and the production performance was greatly restricted by the water block [6, 7]. Therefore, the prediction of saturation becomes the key to the characterization of tight gas reservoirs. This study contributes to the integration of geology and engineering in the exploration and development of tight gas reservoirs [8].

At present, there are two main aspects in the prediction of tight gas reservoir saturation and the optimization of enrichment areas, namely, reservoir petrophysical characterization [9–13] and gas accumulation characteristics [14–18].

Firstly, the reservoir petrophysical characterization is carried out from core to logging interpretation and then to seismic characterization. The research content ranges from microscale pore throat and fluid characteristics [4, 19] to macroscale reservoir distribution. Special core testing, special logging series, seismic attribute fusion, and seismic inversion methods have continuously improved the quantitative degree of research. However, the complexity of tight sandstone gas reservoirs is reflected in the fact that the enrichment areas and petrophysical characteristics of gas reservoirs are not simply correspondences [20]. A large number of high-resistivity intervals produce water, while low-resistivity pay zones produce gas [21]. These features often contradict production performance.

The second is the research on the characteristics of gas accumulation, which mainly covers the type of source rock, the intensity of hydrocarbon generation, the process of gas accumulation [22], and the distribution characteristics of the source rock [23]. The enrichment area is characterized by the relationship between these characteristics and the distribution of the reservoir. Through geochemical experimental analysis, logging interpretation, and seismic prediction, the quality of source rocks, hydrocarbon generation and expulsion process, source-reservoir configuration, and gas migration are described and summarized [24–26]. However, this type of research is usually noticed during the exploration stage. For research purposes and economic benefits, there is usually no further detailed description of gas accumulation characteristics in the development stage, and even the description of source rocks in the static model is usually very brief. This makes the study of gas accumulation characteristics lack quantitative research and the correlation with reservoir characterization. As a result, it is difficult to apply the gas accumulation research work directly to the development practice of tight sandstone gas reservoirs.

In the above research papers, some of the researchers have made attempts to study the saturation height model about low permeability and tight reservoirs [4, 9]. Capillary pressure characteristics, permeability characteristics, and logging interpretation are the research components that have been focused on in these studies. These studies reveal the complexity of low-permeability and tight reservoirs in the spatial distribution of saturation. The saturation height model, a common reservoir characterization method, has much practice in characterizing saturation based on the height above free water level and capillary pressure [27, 28]. In the study of tight sandstone gas reservoirs, further integration of petrophysical characteristics and gas accumulation characteristics is needed to improve the application of the saturation height model.

The above scientific research problems are particularly prominent in the Sulige tight sandstone gas reservoir in the Ordos Basin in northern China, which has been in exploration and development for 20 years. The Sulige tight sandstone gas field belongs to the middle-lower Permian fluvial-delta facies tight sandstone associated with the coalbed [29]. This gas field is currently the largest natural gas field in China [30]. In the long-term production process, the gas-water distribution is complex and the prediction of gas saturation is difficult. These difficulties restrict efficient development in the process of enhanced gas recovery. There

is still a lack of quantitative understanding of the differences in saturation distribution and production water cut in the central, eastern, and western parts of the Sulige gas field. Therefore, this paper attempts to quantitatively analyze the key controlling factors of the saturation distribution characteristics of tight sandstone gas reservoirs by starting with the gas diffusion dynamics and saturation height model and to provide a quantitative interpretation for the gas enrichment areas prediction of Sulige tight sandstone gas reservoir. This is also an attempt to provide a regional approach to geologic modelling to overcome the challenges of spatial prediction of saturation in tight sandstone reservoirs.

## 2. Geological Background

*2.1. Regional Geological Conditions.* Sulige gas field is mainly located in Inner Mongolia and Shaanxi Province, China. It is a giant gas field in China with gas initial in place (GIIP) exceeding one trillion cubic meters [3]. It has the characteristics of a large-scale continuous distribution of tight sandstone gas reservoirs. The effective sand body is small in scale, and the sand body distribution and reservoir petrophysical properties show strong heterogeneity. After 20 years of exploration and development, it is still in the stage of increasing production.

*2.2. Stratigraphic and Structural Characteristics.* The Upper Paleozoic formation in the Sulige gas field is divided from bottom to top into the Carboniferous Benxi Formation, the Permian Taiyuan Formation, Shanxi Formation, Lower Shihezi Formation, Upper Shihezi Formation, and the Shiqianfeng Formation. Among them, the coalbed sets at the top of the Benxi Formation and middle of the Shanxi Formation are widely distributed in the Sulige area and constitute a good regional source rock [31]. The He 8 Member of the Lower Shihezi Formation and the Shan 1 Member of the Shanxi Formation are the main production zones.

The Ordos Basin can be divided into six structural units, the Yimeng uplift, the Weibei uplift, the western Shanxi flexural fold belt, the Yishan slope, the Tianhuan depression, and the western margin thrust belt [32, 33]. The main body of the Sulige gas field is located in the northwest of the Yishan slope (Figure 1). The gas field as a whole is a monoclinical sloping to the southwest, with an inclination angle of less than 1°. Several nose-shaped NE trending uplifts is developed, with a width of 5–8 km, a length of 10–35 km, and an uplift range of 10–25 m.

*2.3. Sedimentary Characteristics.* The Shanxi stage to Shiqianfeng stage in the Ordos Basin belongs to the sedimentary evolution stage dominated by continental facies. In the late Shanxi and early Shihezi stages, the fluvial facies and delta plains were dominant, and the northern margin of the basin had strong tectonic activities and a sufficient supply of debris. Alluvial fan-alluvial plain-delta sedimentary facies developed from north to south, reaching the central and southern parts of the basin (Figure 2). The upper submember of He 8 and Shan 1 Member are meandering river delta deposits [32–37]. The lower submember of He 8 is

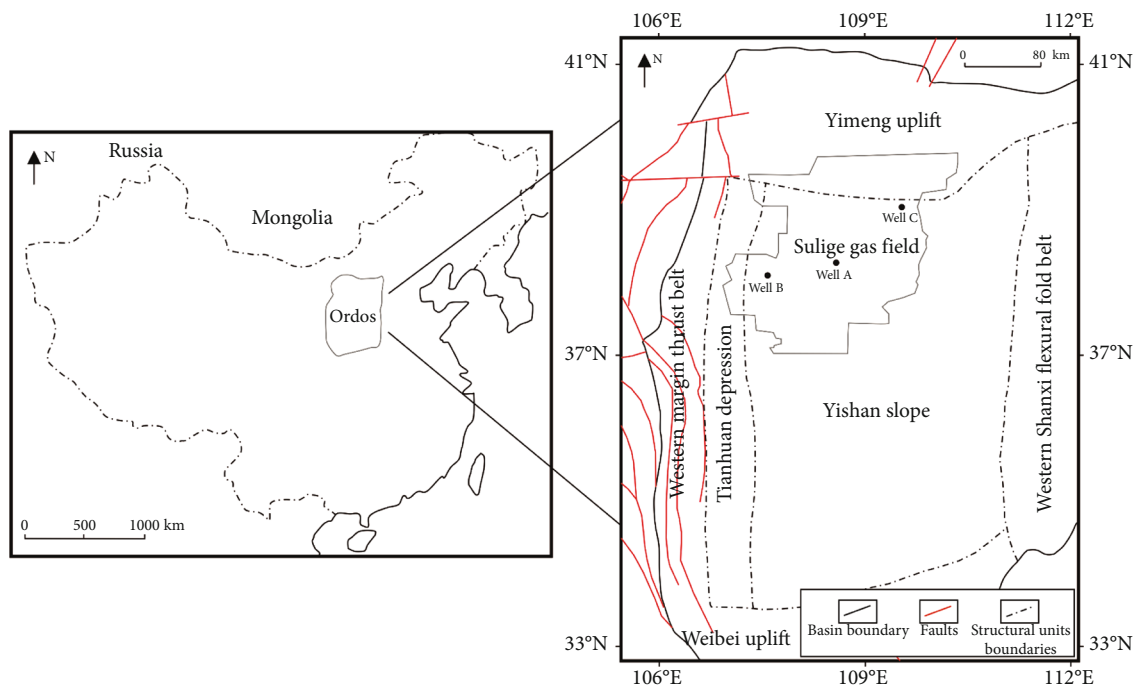


FIGURE 1: The geographical location of research region.

braided river delta [36]. There are three sets of braided river sedimentary systems of northern provenance, which are widely distributed.

#### 2.4. Geological Characteristics of Sulige Tight Sandstone Gas Reservoir

**2.4.1. Low GIIP Abundance.** The GIIP abundance in different segments of the gas reservoir varies greatly. The single flow units are constrained by the multistage fluvial channel lithologic interfaces, which results in poor interwell connectivity and a low single-well controlled GIIP [38].

**2.4.2. Low Porosity and Extralow Permeability.** In general, porosity is distributed in the range of 1% to 15%, with an average of 7%, and air permeability is distributed in the range of 0.01 to 12 mD, with an average of 0.37 mD [39]. The study of reservoir diagenesis, combined with gas migration and accumulation characteristics [22], reflects the “tight earlier and accumulation later” feature of the reservoirs [40].

**2.4.3. Low Formation Pressure Coefficient.** The formation pressure coefficient in the Sulige tight gas reservoir is generally between 0.66 and 0.99 [41].

**2.4.4. The Small Scale of the Effective Sand Body.** The sandstone in the Sulige gas reservoir is distributed throughout the area, controlled by compaction, and the sandstone is generally tight. Effective reservoirs are mainly formed by coarse sandstone and gravel-bearing coarse sandstone. The coarse sandstone is mainly developed in the central bar and the lower part of the channel, and the effective sand body accounts for about 30% of the total thickness of the sandstone. The effective sand bodies are thin in thickness, small in scale, poor in connectivity, developed in multiple stages vertically, staggered

and superimposed, and combined laterally [42]. The effective sand bodies are vertically distributed in each interval, and there is no absolute main pay zone.

**2.4.5. Small Pore Size.** The main pore types in the reservoir include intergranular pores, dissolution pores, and intercrystalline pores, among which dissolution pores develop in debris and matrix. The pore size distribution represents the complexity of mineral composition and its corresponding micropore shape [43].

**2.4.6. Complex Characteristics of Gas Saturation.** Affected by factors such as regional structure, hydrocarbon generation intensity, and reservoir heterogeneity, the gas-bearing properties of different zones are significantly different (Figure 3). The western zone and the northeastern zone have more severe water production and low gas saturation, which are gas-water transition zones. The gas intervals, the gas-water transitional zones, and the water intervals are distributed across each other, with poor continuity and lack of a uniform gas-water contact [44].

### 3. Methods

**3.1. Saturation Height Model of Tight Sandstone Gas Reservoirs.** The saturation height model is generally recommended as the best practice method for saturation characterization and modelling because it describes the hydrocarbon accumulation process with good spatial predictability. Based on the data obtained from the core and logging interpretation, researchers have proposed a number of saturation height models to quantify the characteristics of the saturation distribution. Common methods include the Brooks and Corey method, the Leverett  $J$  method, and the Skelt-

| System        | Series  | Formation     | Thickness (m) | Lithology           | Sedimentary facies       | Source | Reservoir | Seal     | Legend         |           |
|---------------|---------|---------------|---------------|---------------------|--------------------------|--------|-----------|----------|----------------|-----------|
| Permian       | Upper   | Upper Shihezi | 200           | -                   | Shallow lacustrine       |        |           |          | • •            |           |
|               |         |               |               | • •                 |                          |        |           |          | Fine sandstone |           |
|               | Middle  | Lower Shihezi | 100 - 200     | -                   | Fluvial and delta        |        |           | • • •    | Siltstone      |           |
| Carboniferous | Lower   | Shanxi        | 37 - 125      | -                   | Fluvial, delta and swamp |        |           |          | - -            |           |
|               |         |               |               | • •                 |                          |        |           |          | Mudstone       |           |
|               | Taiyuan | 22 - 276      | -             | Restricted platform |                          |        | ▬         | Coal bed |                |           |
| Ordovician    | Lower   | Benxi         | 0 - 40        | -                   | Restricted platform      |        |           |          |                |           |
|               |         | Majiagou      | 100 - 900     | -                   | Platform evaporites      |        |           |          | ▨              | Dolomite  |
|               |         |               |               | -                   | Open platform            |        |           |          | ▧              | Limestone |

FIGURE 2: Stratigraphic column of the research region (modified from [34]).

Harrison method. Common to these methods is that they are used to characterize the buoyancy-driven hydrocarbon charging process that overcomes capillary pressure, transforming the saturation characteristics of the reservoir as a function of rock type, pore size, fluid properties, and hydrocarbon column height, to realize the calculation and prediction of saturation.

**3.1.1. Brooks and Corey Method [45].** The basic data of this method is the reservoir capillary curve data, which is usually obtained by using the mercury injection capillary pressure (MICP). We need to obtain the irreducible water saturation ( $S_{wirr}$ ), the entry capillary pressure ( $PC_e$ ), the capillary pressure ( $PC$ ), and a parameter  $N$  that describes the shape of the capillary pressure curve. The function for the Brooks and Corey method is

$$S_w = S_{wirr} + (1 - S_{wirr}) \cdot \left[ \frac{PC_e}{PC} \right]^{(1/N)}. \quad (1)$$

The method has wide applicability and a clear petrophysical definition. In the process of obtaining saturation, the capillary curve characteristics obtained by the special core analysis (SCAL) are converted into capillary pressure under reservoir conditions by the interfacial tension ( $\sigma$ ) and wetting angle ( $\cos \theta$ ) conversion.

$$(PC)_{res} = (PC)_{lab} \cdot \frac{\sigma_{res} \cdot \cos \theta_{res}}{\sigma_{lab} \cdot \cos \theta_{lab}}. \quad (2)$$

The irreducible water saturation, the entry capillary pressure, and the parameter  $N$  of different rock types of reservoirs can be obtained by curve fitting, and these three parameters can be converted into functions related to porosity. Then, under the condition of equal charging pressure and resistance, the capillary pressure is calculated, so that the corresponding water saturation can be calculated.

**3.1.2. Leverett J Method [46].** The basic data of this method is the reservoir capillary curve data, which is usually obtained by MICP. We need to obtain the capillary pressure and porosity and permeability data. The function of Leverett J's method is expressed as

$$J(S_w) = PC \cdot \sqrt{\frac{K}{\Phi}}. \quad (3)$$

This method has simple and convenient operation, but the disadvantage is that the calculation error of permeability ( $K$ ) will lead to the calculation error of saturation. Corresponding to tight reservoirs, permeability calculation is always a difficult problem. The limitations of test accuracy and logging interpretation methods make the uncertainty of permeability interpretation far greater than that of porosity interpretation. Therefore, the Leverett J method is disadvantaged relative to the Brooks and Corey method in tight reservoirs.

**3.1.3. Skelt-Harrison Method [47].** The basic data of this method is the reservoir capillary curve data, which is usually obtained by using the MICP. We need to obtain the hydrocarbon column height ( $H_r$ ) and the four coefficients of  $A$ ,  $B$ ,  $C$ , and  $D$ . The function of the Skelt-Harrison method is expressed as

$$S_w = 1 - A \cdot e^{-(B/(H_r+D))^C}. \quad (4)$$

The biggest advantage of this method is that it can use a nonlinear way to characterize the heterogeneity of the capillary curve. This method is mostly suitable for carbonate reservoirs with complex pore throat characteristics and significant differences, but not suitable for tight sandstone reservoirs.

**3.2. Gas Diffusion Dynamics in Tight Sandstone Gas Reservoirs.** The mathematical model of gas diffusion dynamics in tight sandstone gas reservoirs is used to describe the nonbuoyancy driving of the gas accumulation process. This

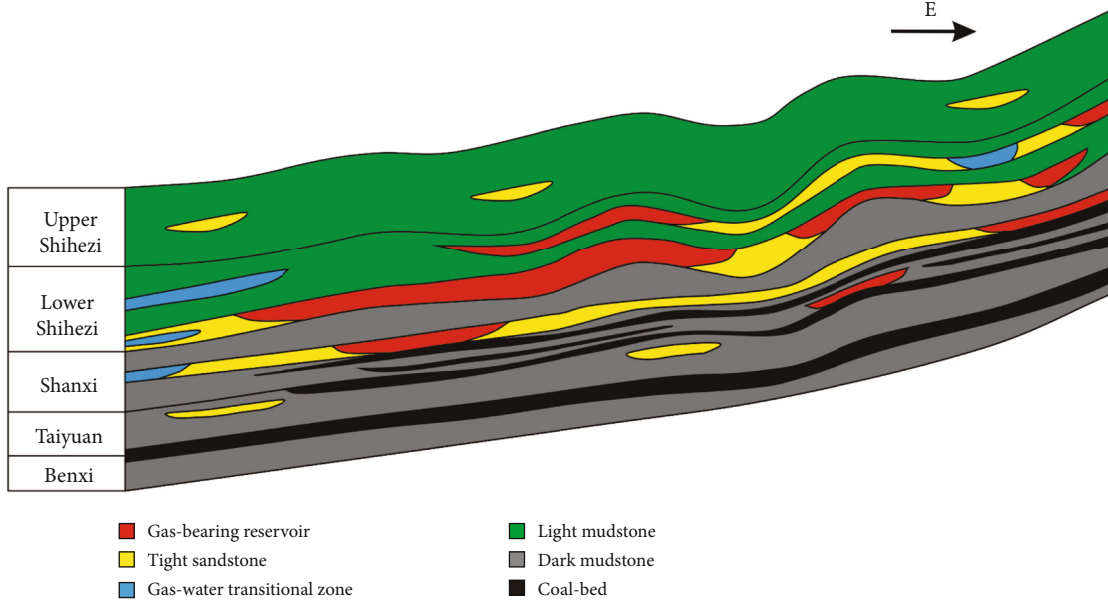


FIGURE 3: Reservoir and source rock distribution section of the research region (modified from [32, 42]).

study is simplified to the diffusion pressure of gas from the source rock, which is used to characterize the hydrocarbon charging process driven by the diffusion pressure to overcome the hydrostatic pressure and capillary pressure. The function is

$$P_{\text{diffusion}} = \frac{z \cdot n \cdot R \cdot T}{V_g} \quad (5)$$

where  $z$  is the deviation factor of gas,  $n$  is the amount of substance (mol),  $R$  is the molar gas constant (8.314 J/(mol·K)),  $T$  is the thermodynamic temperature (K), and  $V_g$  is the gas volume ( $\text{m}^3$ ). The parameter  $n$  describes the ratio of the gas mass to the molar mass ( $M$ , kg/mol), and the gas mass is equal to the gas expulsion intensity ( $q_e$ ,  $10^8 \text{ m}^3/\text{km}^2$ ) multiplied by the area of gas expulsion area ( $S$ ,  $\text{km}^2$ ) and the gas density ( $\rho_g$ ,  $\text{kg}/\text{m}^3$ ).  $V_g$  equals the product of the gas expulsion area ( $S$ ,  $\text{km}^2$ ), the thickness of the source rocks ( $h_s$ , m), and the porosity of the source rocks ( $\phi_s$ , dimensionless).

Therefore, the gas diffusion dynamics function is as follows:

$$P_{\text{diffusion}} = \frac{z \cdot q_e \cdot S \cdot \rho_g \cdot R \cdot T}{M \cdot S \cdot h_s \cdot \Phi_s} \quad (6)$$

In the case where the hydrocarbon source rock and the reservoir are widely and closely connected, the gas charging pressure is the sum of diffusion and buoyancy, while the gas charging resistance is the sum of hydrostatic pressure and capillary pressure. The function is expressed as

$$\frac{z \cdot q_e \cdot \rho_g \cdot R \cdot T}{M \cdot h_s \cdot \Phi_s} + (\rho_w - \rho_g) \cdot g \cdot H_r = PC + \rho_w \cdot g \cdot H. \quad (7)$$

where  $\rho_w$  is water density ( $\text{kg}/\text{m}^3$ ),  $g$  is the gravitational acceleration ( $\text{m}/\text{s}^2$ ),  $H_r$  is gas column height in the reservoir (m), and  $H$  is hydrostatic column height (m).

When the Brooks and Corey method is used to characterize the relationship between capillary pressure and saturation under reservoir conditions, the function is the following:

$$S_w = S_{\text{wirr}} + (1 - S_{\text{wirr}}) \cdot \left( \frac{PC_e}{\left( \frac{z \cdot q_e \cdot \rho_g \cdot R \cdot T}{M \cdot h_s \cdot \Phi_s} + (\rho_w - \rho_g) \cdot g \cdot H_r - \rho_w \cdot g \cdot H \right) \cdot \frac{\sigma_{\text{res}} \cdot \cos \theta_{\text{res}}}{\sigma_{\text{lab}} \cdot \cos \theta_{\text{lab}}}} \right)^{(1/N)} \quad (8)$$

## 4. Results

**4.1. Selection of Research Subjects.** The cored wells A, B, and C in the central, western, and eastern regions of the Sulige

tight sandstone gas field were selected correspondingly for the obvious differences in saturation distribution and production water cut. These wells have routine core analysis, mercury injection capillary pressure, hydrocarbon source

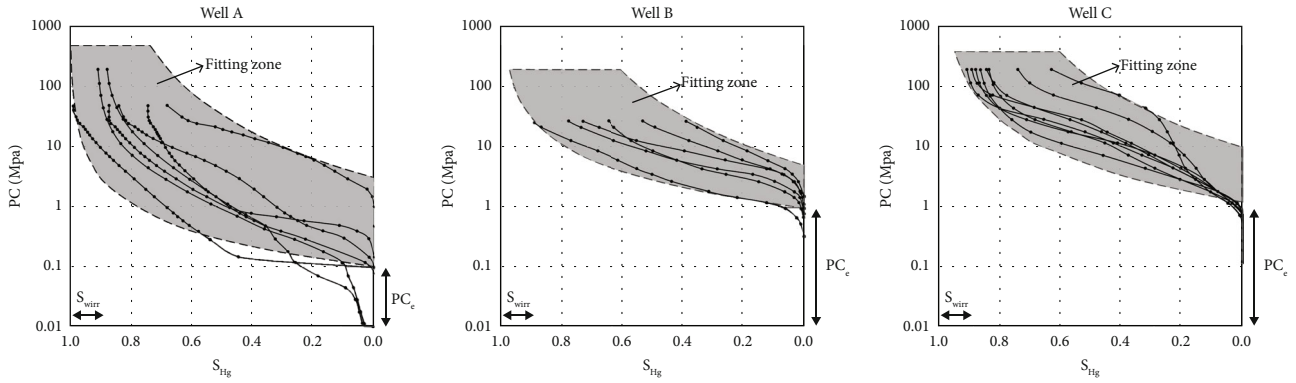


FIGURE 4: Comparison of the saturation height model and MICP data under experiment conditions.

rock quality experiment, pressure volume temperature (PVT) test of gas and formation water, and conventional logging interpretation. The information from these wells can be used for saturation height model and comparison.

In order to verify the effectiveness of the saturation height model for noncoring wells, an additional newly drilled well was selected for model application.

#### 4.2. Parameter Determination of Saturation Height Model.

The parameters involved in the saturation height model mainly include irreducible water saturation ( $S_{wirr}$ ), entry capillary pressure ( $PC_e$ ), shape parameter of capillary pressure curve ( $N$ ), formation water density under gas reservoir conditions ( $\rho_w$ ), natural gas density under gas reservoir conditions ( $\rho_g$ ), gravitational acceleration ( $g$ ), and gas column height ( $H_r$ ). The parameters are as follows:

- (1) The irreducible water saturation parameter is obtained from the experimental results of MICP, nuclear magnetic resonance movable fluid test, and relative permeability endpoint test. Based on the difference in sample porosity, the linear relationship between  $S_{wirr}$  and reservoir porosity is established
- (2) The entry capillary pressure parameter is derived from MICP. According to the difference of sample porosity, the exponential relationship between  $PC_e$  and reservoir porosity is established
- (3) The shape parameter of the capillary pressure curve is derived from MICP. On the basis of the difference in sample porosity, the linear relationship between  $N$  and reservoir porosity is established
- (4) The formation water density under gas reservoir conditions is obtained from PVT tests of formation water. According to the difference between salinity, formation pressure, and temperature in the study area, the value is between 0.96 and  $1.05 \times 10^3 \text{ kg/m}^3$
- (5) The gas density under gas reservoir conditions is derived from the PVT tests of natural gas samples,

and the value is between  $0.45$  and  $0.60 \times 10^3 \text{ kg/m}^3$  according to the difference in the gas components, formation pressure, and temperature in the study area

- (6) The acceleration of gravity is  $9.8 \text{ m/s}^2$
- (7) The gas column height is obtained from the regional structural characteristics and reservoir thickness

When these three parameters of  $S_{wirr}$ ,  $PC_e$ , and  $N$  are determined, the fit between the capillary pressure and the mercury saturation for the experimental conditions can be completed (Figure 4). By converting the interfacial tension of air-mercury to that of gas-brine, the capillary curve and the fitting result under experimental conditions can be converted to that under gas reservoir conditions (Figure 5), and the saturation height model is carried out.

#### 4.3. Determination of Parameters of Gas Diffusion Dynamics.

The parameters involved in gas diffusion dynamics mainly include the natural gas deviation factor ( $z$ ), the gas expulsion intensity ( $q_e$ ), the molar gas constant ( $R$ ), the thermodynamic temperature ( $T$ ), the natural gas molar mass ( $M$ ), source rock thickness ( $h_s$ ), and source rock porosity ( $\phi_s$ ). The parameters for obtaining the parameters are as follows:

- (1) The parameter of the natural gas deviation coefficient is derived from the analysis of natural gas components, and the value is between 0.90 and 1.00 according to the Standing-Katz chart analysis
- (2) The gas expulsion intensity is derived from the experiment results of the hydrocarbon generation and expulsion of the source rocks, and its value ranges from  $12$  to  $26 \times 10^8 \text{ m}^3/\text{km}^2$ , which is related to the coalbed, dark mudstone, and their maturity
- (3) The molar gas constant is  $8.314 \text{ J}/(\text{mol}\cdot\text{K})$
- (4) The thermodynamic temperature parameter is obtained from the results of the formation temperature test, and the value is between 353 and 398 K
- (5) The molar mass of natural gas is  $16 \text{ kg/mol}$

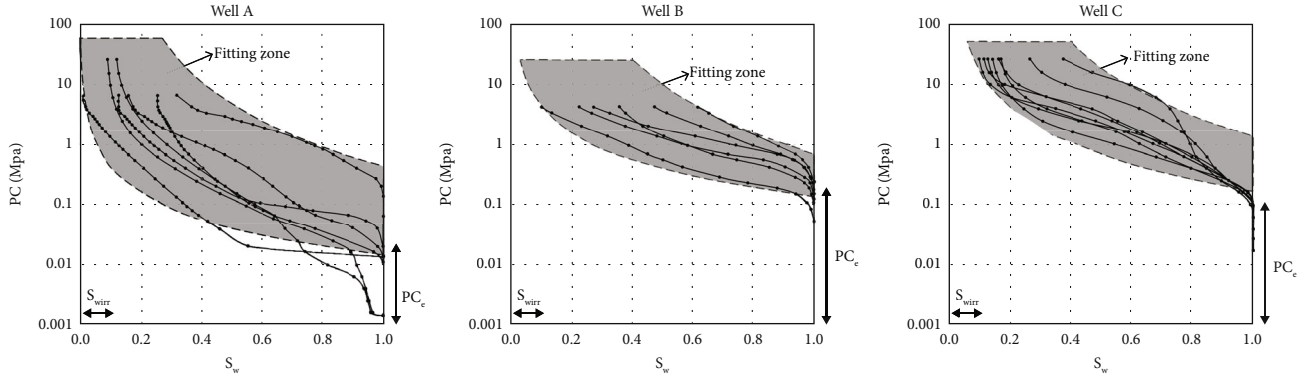


FIGURE 5: Comparison of the saturation height model and MICP data under reservoir conditions.

TABLE 1: Table of gas diffusion parameters obtained from cored wells.

| Well | $z$   | $q_e$ ( $10^8 \text{ m}^3/\text{km}^2$ ) | $R$ (J/(mol·K)) | $T$ (K) | $\rho_g$ ( $\text{kg}/\text{m}^3$ ) | $M$ (kg/mol) | $h_s$ (m) | $\varphi_s$ | $H$ (m) | $\rho_w$ ( $\text{kg}/\text{m}^3$ ) |
|------|-------|------------------------------------------|-----------------|---------|-------------------------------------|--------------|-----------|-------------|---------|-------------------------------------|
| A    | 0.960 | 18.2                                     | 8.314           | 380     | 492                                 | 16           | 145       | 0.0352      | 3330    | 1000                                |
| B    | 0.975 | 14.3                                     | 8.314           | 389     | 541                                 | 16           | 125       | 0.0340      | 3550    | 990                                 |
| C    | 0.950 | 20.9                                     | 8.314           | 363     | 540                                 | 16           | 115       | 0.0436      | 2900    | 1100                                |

- (6) The source rock thickness parameter is obtained from the results of the logging interpretation, which are the sum of dark mudstone and the coalbed thicknesses, and the value is between 70 and 180 m
- (7) The source rock average porosity parameter is obtained from the core test and logging interpretation results which are the weighted average porosity of dark mudstone and coalbed, and the value is between 0.02 and 0.05

Furthermore, the hydrostatic column pressure, which is the resistance, is obtained by calculating the hydrostatic column height ( $H$ ) based on the vertical depth.

The parameters of the two cored wells in the study area are shown in Table 1.

**4.4. Calculation Results and Data Verification.** According to the results of the log interpretation and experimental results, the saturation of the wells is calculated, which is compared to the logging interpretation results of the log interpretation of the Archie's law. The comparison results show that the calculation results of the new model are consistent with the trend of Archie's interpretation (Figures 6, 7, and 8), and the gas-water identification is accurate by production performance.

The saturation height model 1 (orange line) in Figures 6 and 7 converts the parameters into a function of porosity, and a comparison of the saturation height model and Archie's interpretation shows that the error is mainly within  $\pm 4\%$ . For the analysis of reservoir intervals outside this range (Figure 8), two main reasons can be found. The first is that in reservoir intervals with relatively high shale volumes, the relationship between porosity and saturation changes due to the rock type, which in turn causes differences in the saturation height model and Archie's interpretation. By con-

verting the parameters of the SHM into a function of porosity and rock type to form the saturation height model 2 (green line), the fitting effect is significantly improved. However, the presence of calcareous cement at the top and bottom of some reservoir intervals leads to unusually high resistivity, which in turn leads to deviations in the saturation interpretation.

A newly drilled noncoring well around well B was selected as an example (Figure 9). The well has two sets of logging sequences, lateral resistivity and array-induced resistivity. The saturation height model (SHM) predictions are mostly within the range of the two sets of resistivity interpretation results. This indicates that the saturation height model can be reliable on noncoring wells and can be extended to the entire study area in terms of saturation prediction.

**4.5. Uncertainty Analysis and Quality Control.** There are numerous parameters in the saturation height model presented in the current study. Different data sources lead to differences in the uncertainty ranges of the parameters. The uncertainties may arise from experimental errors, sample representativeness, logging interpretation, etc. For example, the deviation factor of gas ( $z$ ) and gas density ( $\rho_g$ ) are controlled by the formation pressure ( $P$ ), the temperature ( $T$ ), and the gas components; then,  $z$  is collinear with  $\rho_g$ . In the following figure, the parameters are listed in order according to their collinearity and correlation, and the sources and ranges of uncertainty for different parameters are analyzed, respectively (Figure 10).

Based on the tornado plot analysis, the source rock parameters are the most dominant uncertainty factor, such as gas expulsion intensity, source rock thickness, and source rock porosity. The uncertainty of this factor mainly comes from three aspects: (1) the data of gas expulsion intensity are obtained from core experiments with the limited number

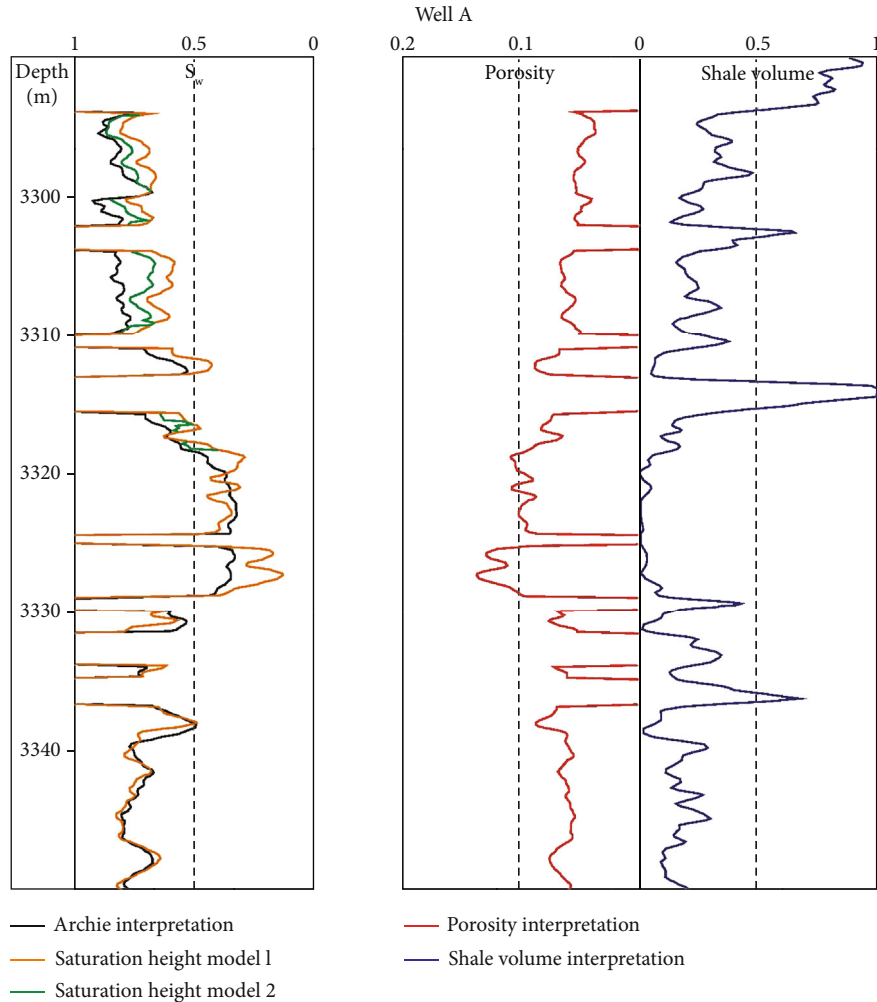


FIGURE 6: Comparison of the results of the saturation height model and Archie's interpretation in well A.

of coring wells; (2) the calculation method of source parameters by noncoring wells is to discriminate the thickness of coalbed and dark mudstone by logging lithology interpretation; and (3) the spatial prediction is mainly based on seismic data and geostatistical simulation. Errors in the core-log calibration process may lead to an increase in uncertainty. In particular, it is very difficult to predict the thickness of the thinner coalbed based on seismic data alone.

To cope with the uncertainty in the estimation of gas expulsion intensity and other related parameters related to gas accumulation, quality control is carried out from three aspects: (1) relying on a large amount of well data in the study area, based on logging and mud-logging interpretation to improve the characterization accuracy [48]; (2) referring to other characterization methods of gas expulsion to improve the calculation accuracy, such as mudstone compaction regression by logging acoustic curves to calculate the excess formation pressure. In a tight gas reservoir, the value of under pressure is quantitatively related to gas saturation [49]; and (3) with abundant data available, statistical simulation methods such as Monte Carlo are used to estimate the parameters [50].

## 5. Discussion

**5.1. Determination of the Lower Limit of Gas Charging.** Based on the results of the saturation height model, the theoretical lower limit of charging is whether the charging pressure can exceed the entry capillary pressure. Under the condition of the average entry capillary pressure in different part of studying area, the gas expulsion intensity should reach approximately  $13 \times 10^8 \text{ m}^3/\text{km}^2$  in central and western area before the charging can be started. In the east, it should reach more than  $17 \times 10^8 \text{ m}^3/\text{km}^2$ .

However, this lower limit is not directly applicable to actual geological design and production, because the impact on production performance is severe if hydraulic fracturing perforated into the transition zone with moveable formation water. For example, a poor gas formation with high entry capillary pressure and high gas expulsion intensity may be numerically similar to a poor gas formation with low entry capillary pressure and low gas expulsion intensity, but the production performances are completely different. Such detailed work must be integrated with theoretical results and specific development scenarios.



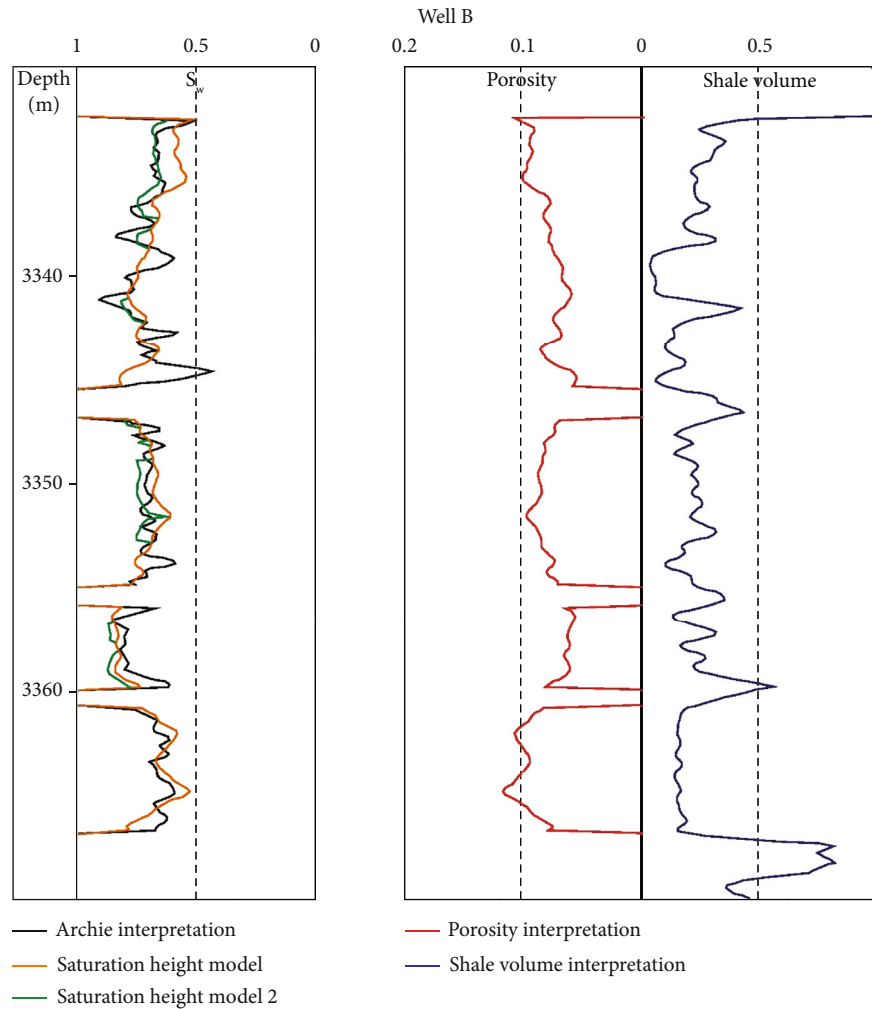


FIGURE 7: Comparison of the results of the saturation height model and Archie's interpretation in well B.

5.2. Controlling Factors of Saturation in Tight Sandstone.

The tight gas reservoirs in the study area have the characteristics of wide and gentle structure, which lead to lower gas column height and higher capillary resistance, making it impossible to displace formation water only by buoyancy, thus forming a large area gas-water transition zone. The spatial distribution of the saturation features is complex.

The tight gas reservoirs in the study area are in close contact with the source rock. During the structural evolution of the basin, the gas migration paths such as faults and high-permeability layers are not developed. Gas migration depends mainly on vertical and lateral gas diffusion in short distances. The gas diffusion pressure directly controls whether natural gas can overcome capillary pressure to charge into the reservoir.

The geological characteristics and production performances show that there is an obvious correlation between the intensity of hydrocarbon generation and the gas saturation, and the horizontal difference of the hydrocarbon generation controls the horizontal difference of the gas-water distribution.

The sedimentary characteristics of fluvial facies make the spatial distribution of sand bodies complex, and the differences in reservoir architecture mainly control the reservoir

heterogeneity. The gas-water distribution is controlled by these features. The sand bodies under the control of the two main types of sedimentary facies, the central bar and the fluvial channel, have the characteristics of coarsening upward and finer grain size, respectively. The reservoir heterogeneity in the central bar is relatively weak, and the pore size is better than the fluvial channel, which makes the gas saturation higher in larger-scale or multistage superimposed central bar, while the channel sand body generally has the characteristics of a gas-water transition, or the bottom is gas and the top is water.

The regional tiny uplift structure can improve gas saturation. The high part of the uplift with the good quality sand body will further improve the gas saturation characteristics.

Differences in sedimentary sources and diagenesis in the study area lead to differences in the content and composition of rock minerals and clay minerals. These differences affect reservoir quality in the first place, with high clay mineral content and poor particle sorting generally corresponding to poorer reservoir quality, which in turn reduces gas saturation. More importantly, the difference in the content and composition of rock and clay minerals will significantly affect the wettability of the reservoir, and stronger

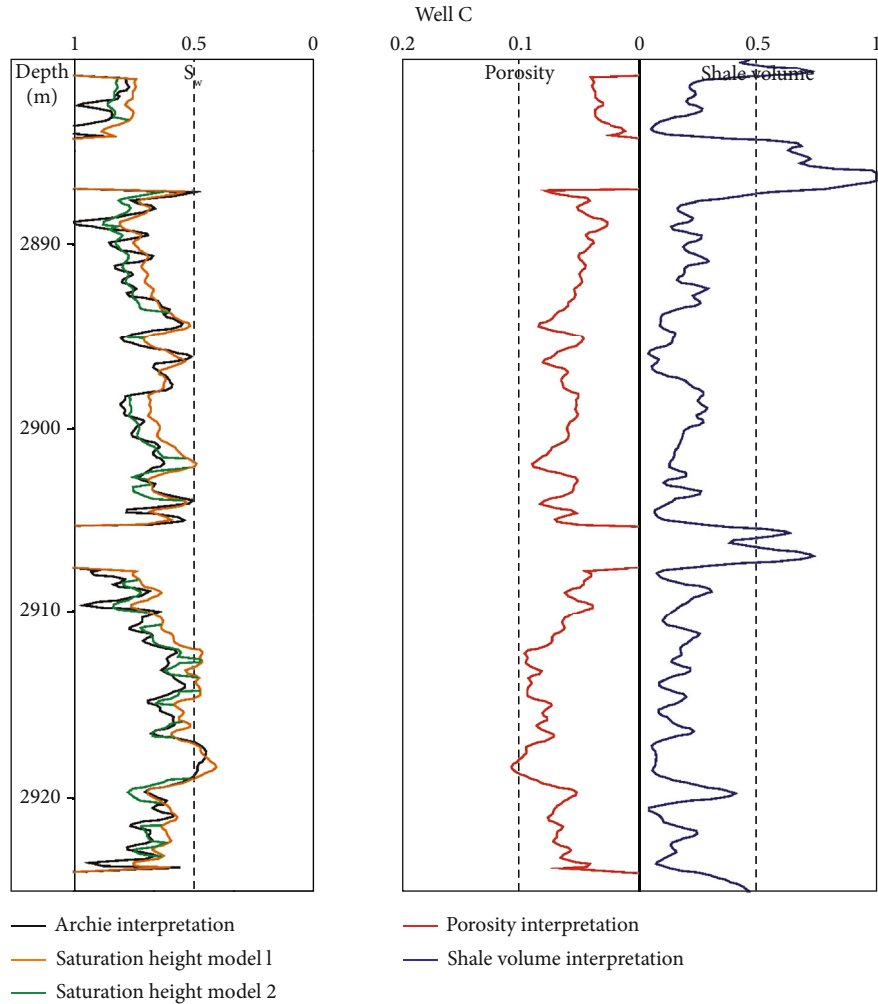


FIGURE 8: Comparison of the results of the saturation height model and Archie's interpretation in well C.

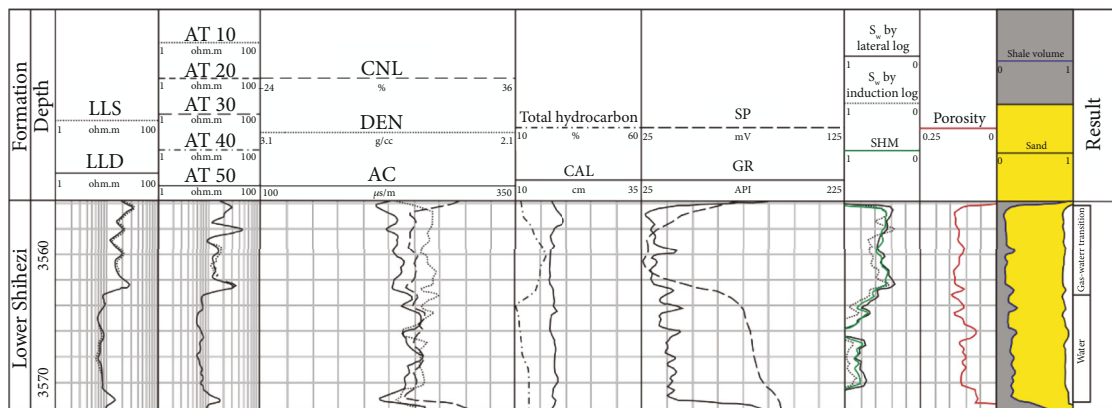


FIGURE 9: Column of saturation height interpretation results for noncored well.

hydrophilicity will increase the resistance of gas charging, resulting in a decrease in gas saturation.

These characteristics mentioned above explain why there is a significant difference in saturation distribution and production water cut in the central, western, and eastern parts

of the Sulige gas field. As shown in well A geological characteristics and saturation interpretation results, the source rocks in the central region are high in expulsion intensity, the coalbed especially is in close contact with the reservoir, and the reservoir quality is generally good, so the production

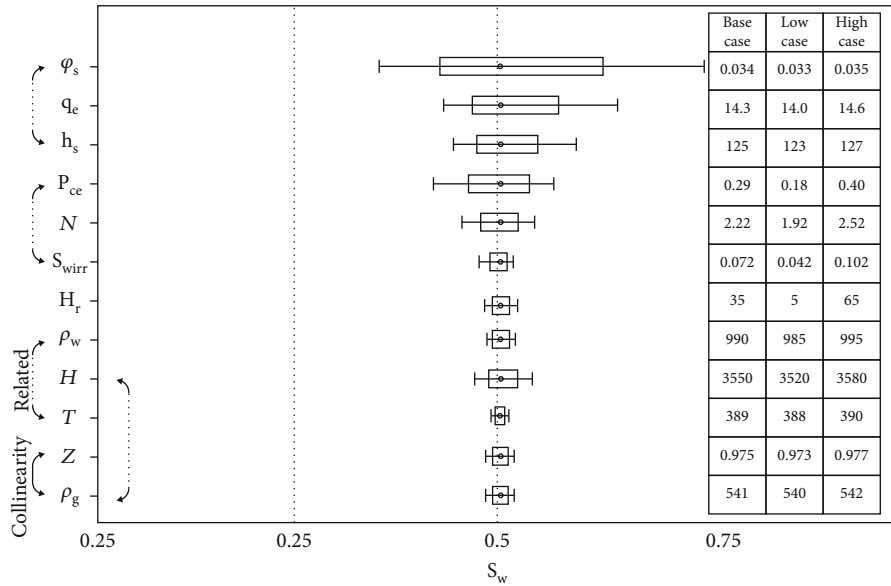


FIGURE 10: Tornado plots for different parameter uncertainty ranges in well B.

performance is good without water cut. As shown in well B, the source rocks in the western region are low in expulsion intensity, and the reservoir quality is heterogeneity, so a large gas-water transition zone is formed, and the local uplift or the area with good reservoir properties is prone to good production performance but high water cut. As shown in well C, the source rocks in the eastern region are high in expulsion intensity, and the sands are thick but mostly tight, making the production performance generally poor.

The consistency of the saturation calculation results with the logging interpretation confirmed the accuracy of the gas diffusion dynamics and the saturation height model and provided a basis for saturation modelling and prediction.

**5.3. Application of the New Saturation Height Model to Static Models.** The application of the new function in the static model presumes that the structural model, rock type (facies) model, and porosity model are reliably established. The quality control requirements for these three types of models are as follows:

The structural model grid is valid, the structural interpretation of the horizons is accurate, the well tops and seismic interpretation are consistent, and the “bull eye” of structural errors is avoided. The grid height of the source rock formation can be set finer, because it is not involved in the numerical simulation and does not worry about the computational rate. This can make the thin layers in the source rock modelling more detailed.

The requirements for rock type (facies) modelling are divided into reservoir facies modelling and source rock facies modelling. Geometric morphological characterization of sand bodies of different genesis is performed in reservoir facies modelling. Based on the differences in their petrophysical characteristics, they are classified into rock types with significant differences in porosity, permeability, and capillary characteristics, and the precision of saturation calculation

can be improved by modifying the function proposed in this paper in different rock types. It is necessary to consider the facies and rock type modelling of the source rock. As described in Section 4.5, to improve the modelling accuracy of source rock facies and rock types, the focus is on integrated characterization using multidisciplinary data such as cores, logs, mud logs, and seismic, under geostatistical and neural network learning methods.

The porosity model mainly relies on the data from core calibration logging interpretation. In this study area, the seismic inversion data only play a trend constraint role for the porosity model due to the limitation of seismic data resolution and reservoir thickness. Quality control of log interpretation, especially porosity correction of mudstone and borehole anomaly sections, can greatly improve the progress of porosity modelling.

After completing quality control of the structural model, rock type (facies) model, and porosity model, the new saturation height model is conveniently applied. The saturation model can be obtained by bringing the above models into the function and using geometric model calculations, and then, model corrections are made to achieve a better fit based on feedback from uncertainty analysis and numerical simulation work.

## 6. Conclusions

Taking gas diffusion dynamics into account, this study extends a saturation height model to calculate and discriminate the saturation of tight sandstone gas reservoirs. Using this model, the saturation distribution of gas-bearing sandstones can be quantitatively interpreted when studying tight reservoirs with complex saturation distributions and reservoir capillary resistance much greater than buoyancy.

By applying this model to the Sulige tight gas reservoir, this study concludes that the configuration between gas

diffusion dynamics and reservoir capillary pressure controls the distribution of saturation. The buoyancy effect only serves to improve the saturation at regional uplifts with good petrophysical properties. The different saturation characteristics in the central, western, and eastern parts of the Sulige area are precisely caused by the different configurations of source rock quality and reservoir quality. This is reflected in the difference between two key parameters, gas expulsion intensity and the entry capillary pressure. Other source rock parameters and reservoir parameters also play a part in the impact. This saturation height model can provide critical information to guide the geologic design of the development plan and calculations of tight sandstone gas saturation in the static model.

### Data Availability

The data is already included within the manuscript.

### Conflicts of Interest

The authors declare that they have no conflicts of interest.

### Acknowledgments

This study was funded by the Youth Innovation Project in Research Institute of Petroleum Exploration and Development, CNPC (no. 2021-40234-000039). We gratefully thank the Sulige Development Branch of Changqing Oilfield of CNPC for their permission to publish this work.

### References

- [1] L. Sun, C. Zou, A. Jia et al., "Development characteristics and orientation of tight oil and gas in China," *Petroleum Exploration and Development*, vol. 46, no. 6, pp. 1073–1087, 2019.
- [2] H. Huang, R. Li, F. Xiong et al., "A method to probe the pore-throat structure of tight reservoirs based on low-field NMR: insights from a cylindrical pore model," *Marine and Petroleum Geology*, vol. 117, article 104344, 2020.
- [3] L. Li, "Development of natural gas industry in China: review and prospect," *Natural Gas Industry B*, vol. 9, no. 2, pp. 187–196, 2022.
- [4] K. W. Shanley and R. M. Cluff, "The evolution of pore-scale fluid-saturation in low-permeability sandstone reservoirs," *AAPG Bulletin*, vol. 99, no. 10, pp. 1957–1990, 2015.
- [5] J. A. Masters, "Deep basin gas trap, Western Canada," *AAPG Bulletin*, vol. 63, no. 2, pp. 152–181, 1979.
- [6] J. Mahadevan and M. M. Sharma, "Factors affecting cleanup of water blocks: a laboratory investigation," *SPE Journal*, vol. 10, no. 3, pp. 238–246, 2005.
- [7] H. Huang, R. Li, Z. Lyu et al., "Comparative study of methane adsorption of Middle-Upper Ordovician marine shales in the western Ordos basin, NW China: insights into impacts of moisture on thermodynamics and kinetics of adsorption," *Chemical Engineering Journal*, vol. 446, article 137411, 2022.
- [8] S. Xu, F. Yang, Z. Feng, R. Liu, and G. Lei, "Editorial: advances in the exploration and development of unconventional oil and gas: from the integration of geology and engineering," *Economic Geology*, vol. 10, article 930704, 2022.
- [9] S. Rudyk and A. Al-Lamki, "Saturation-height model of Omani deep tight gas reservoir," *Journal of Natural Gas Science and Engineering*, vol. 27, pp. 1821–1833, 2015.
- [10] W. Tian, A. Li, X. Ren, and Y. Josephine, "The threshold pressure gradient effect in the tight sandstone gas reservoirs with high water saturation," *Fuel*, vol. 226, no. 15, pp. 221–229, 2018.
- [11] X. Zhou, C. Zhang, Z. Zhang, R. Zhang, L. Zhu, and C. Zhang, "A saturation evaluation method in tight gas sandstones based on diagenetic facies," *Marine and Petroleum Geology*, vol. 107, pp. 310–325, 2019.
- [12] A. Soleymanzadeh, A. Helalizadeh, M. Jamialahmadi, and B. S. Soulgani, "Development of a new model for prediction of cementation factor in tight gas sandstones based on electrical rock typing," *Journal of Natural Gas Science and Engineering*, vol. 94, article 104128, 2021.
- [13] Q. Qi, L. Fu, J. Deng, and J. Cao, "Attenuation methods for quantifying gas saturation in organic-rich shale and tight gas formations," *Geophysics*, vol. 86, no. 2, pp. D65–D75, 2021.
- [14] J. Wood, "Water distribution in the Montney tight gas play of the Western Canadian Sedimentary basin: significance for resource evaluation," *SPE Reservoir Evaluation & Engineering*, vol. 16, no. 3, pp. 290–302, 2013.
- [15] D. R. Spain, G. Merletti, M. Webster, and L. Kaye, *The Importance of Saturation History for Tight Gas Deliverability*, SPE-163958-MS, 2013.
- [16] F. Jiang, X. Pang, F. Guo, and J. Guo, "Critical conditions for natural gas charging and delineation of effective gas source rocks for tight sandstone reservoirs," *Geological Journal*, vol. 51, no. 1, pp. 113–124, 2016.
- [17] M. H. Doranehgard, S. Tran, and H. Dehghanpour, "Modeling of natural-gas diffusion in oil-saturated tight porous media," *Fuel*, vol. 300, article 120999, 2021.
- [18] Z. Liu, S. Guo, Y. Huang, Z. Cao, T. Yeerhazi, and W. Cao, "The tight sand reservoir characteristics and gas source in coal measures: a case study of typical areas in China," *Geofluids*, vol. 2022, Article ID 4983334, 17 pages, 2022.
- [19] H. Huang, R. Li, W. Chen et al., "Revisiting movable fluid space in tight fine-grained reservoirs: a case study from Shahejie shale in the Bohai Bay basin, NE China," *Journal of Petroleum Science & Engineering*, vol. 207, article 109170, 2021.
- [20] A. Sakhaee-Pour and S. L. Bryant, "Effect of pore structure on the producibility of tight-gas sandstones," *AAPG Bulletin*, vol. 98, no. 4, pp. 663–694, 2014.
- [21] Y. Jiang, J. Zhou, X. Fu, L. Cui, C. Fang, and J. Cui, "Analyzing the origin of low resistivity in gas-bearing tight sandstone reservoir," *Geofluids*, vol. 2021, Article ID 4341804, 15 pages, 2021.
- [22] J. Li, J. Zhao, X. Wei et al., "Gas expansion caused by formation uplifting and its effects on tight gas accumulation: a case study of Sulige gas field in Ordos basin, NW China," *Petroleum Exploration and Development*, vol. 49, no. 6, pp. 1266–1281, 2022.
- [23] W. Ji, F. Hao, H. Schulz, Y. Song, and J. Tian, "The architecture of organic matter and its pores in highly mature gas shales of the lower Silurian Longmaxi formation in the Upper Yangtze platform, South China," *AAPG Bulletin*, vol. 102, no. 12, pp. 2909–2942, 2019.
- [24] J. Dai, Y. Ni, and X. Wu, "Tight gas in China and its significance in exploration and exploitation," *Petroleum Exploration and Development*, vol. 39, no. 3, pp. 277–284, 2012.

- [25] L. Chen, Z. Jiang, Q. Liu et al., "Mechanism of shale gas occurrence: insights from comparative study on pore structures of marine and lacustrine shales," *Marine and Petroleum Geology*, vol. 104, pp. 200–216, 2019.
- [26] K. Zhang, Y. Song, C. Jia et al., "Formation mechanism of the sealing capacity of the roof and floor strata of marine organic-rich shale and shale itself, and its influence on the characteristics of shale gas and organic matter pore development," *Marine and Petroleum Geology*, vol. 140, article 105647, 2022.
- [27] M. O. Amabeoku, D. G. Kersey, R. H. Bin Nasser, and A. R. Al-Belawi, "Relative permeability coupled saturation-height models on the basis of hydraulic (flow) units in a gas field," *SPE Reservoir Evaluation & Engineering*, vol. 11, no. 6, pp. 1013–1028, 2008.
- [28] A. Abdollahian, M. Tadayoni, and R. Bin Junin, "A new approach to reduce uncertainty in reservoir characterization using saturation height modeling, Mesaverde tight gas sandstones, western US basins," *Journal of Petroleum Exploration and Production Technology*, vol. 9, no. 3, pp. 1953–1961, 2019.
- [29] C. Zou, Z. Yang, S. Huang et al., "Resource types, formation, distribution and prospects of coal-measure gas," *Petroleum Exploration and Development*, vol. 46, no. 3, pp. 451–462, 2019.
- [30] X. Ma, "Extreme utilization' development theory of unconventional natural gas," *Petroleum Exploration and Development*, vol. 48, no. 2, pp. 381–394, 2021.
- [31] Y. Li, A. Fan, R. Yang, Y. Sun, and N. Lenhardt, "Braided deltas and diagenetic control on tight sandstone reservoirs: a case study on the Permian Lower Shihezi formation in the southern Ordos basin (Central China)," *Marine and Petroleum Geology*, vol. 435, article 15106156, 2022.
- [32] H. Yang and X. Liu, "Progress in Paleozoic coal-derived gas exploration in the Ordos basin, West China," *Petroleum Exploration and Development*, vol. 41, no. 2, pp. 144–152, 2014.
- [33] W. Ji, Y. Song, Z. Jiang, X. Wang, Y. Bai, and J. Xing, "Geological controls and estimation algorithms of lacustrine shale gas adsorption capacity: a case study of the Triassic strata in the southeastern Ordos basin, China," *International Journal of Coal Geology*, vol. 134–135, pp. 61–73, 2014.
- [34] Y. Yang, W. Li, and L. Ma, "Tectonic and stratigraphic controls of hydrocarbon systems in the Ordos basin: a multicycle cratonic basin in Central China," *AAPG Bulletin*, vol. 89, no. 2, pp. 255–269, 2005.
- [35] H. Huang, R. Li, Z. Jiang, J. Li, and L. Chen, "Investigation of variation in shale gas adsorption capacity with burial depth: insights from the adsorption potential theory," *Journal of Natural Gas Science & Engineering*, vol. 73, article 103043, 2020.
- [36] Y. Li, A. Fan, R. Yang, Y. Sun, and N. Lenhardt, "Sedimentary facies control on sandstone reservoir properties: a case study from the Permian Shanxi formation in the southern Ordos basin, central China," *Marine and Petroleum Geology*, vol. 129, article 105083, 2021.
- [37] B. Zhao, R. Li, X. Qin et al., "Geochemical characteristics and mechanism of organic matter accumulation of marine-continental transitional shale of the Lower Permian Shanxi formation, southeastern Ordos basin, North China," *Journal of Petroleum Science & Engineering*, vol. 205, article 108815, 2021.
- [38] X. Ma, A. Jia, J. Tan, and D. He, "Tight sand gas development technology and practices in China," *Petroleum Exploration and Development*, vol. 39, no. 5, pp. 611–618, 2012.
- [39] X. Lin, J. Zeng, J. Wang, and M. Huang, "Natural gas reservoir characteristics and non-Darcy flow in low-permeability sandstone reservoir of Sulige gas field, Ordos basin," *Energies*, vol. 13, no. 7, p. 1774, 2020.
- [40] H. Yang, J. Fu, X. Liu, and P. Meng, "Accumulation conditions and exploration and development of tight gas in the Upper Paleozoic of the Ordos basin," *Petroleum Exploration and Development*, vol. 39, no. 3, pp. 315–324, 2012.
- [41] H. Xu, D. Tang, J. Zhang, W. Yin, W. Zhang, and W. Li, "Factors affecting the development of the pressure differential in Upper Paleozoic gas reservoirs in the Sulige and Yulin areas of the Ordos basin, China," *International Journal of Coal Geology*, vol. 85, no. 1, pp. 103–111, 2011.
- [42] D. He, L. Wang, G. Ji, Y. Wei, and C. Jia, "Well spacing optimization for Sulige tight sand gas field, NW China," *Petroleum Exploration and Development*, vol. 39, no. 4, pp. 491–497, 2012.
- [43] Z. Wang, X. Jiang, M. Pan, and Y. Shi, "Nano-scale pore structure and its multi-fractal characteristics of tight sandstone by N<sub>2</sub> adsorption/desorption analyses: a case study of Shihezi formation from the Sulige gas field, Ordos basin, China," *Minerals*, vol. 10, no. 4, p. 377, 2020.
- [44] D. Meng, A. Jia, G. Ji, and D. He, "Water and gas distribution and its controlling factors of large scale tight sand gas fields: a case study of western Sulige gas field, Ordos basin, NW China," *Petroleum Exploration and Development*, vol. 43, no. 4, pp. 663–671, 2016.
- [45] R. H. Brooks and A. T. Corey, "Hydraulic properties of porous media," in *Hydrology*, pp. 3–27, Colorado State University Press, 1964.
- [46] M. C. Leverett, "Capillary behavior in porous solids," *Petroleum Transactions, AIME*, vol. 142, no. 1, pp. 152–169, 1941.
- [47] C. Skelt and R. Harrison, "An integrated approach to saturation height analysis," in *SPWLA, 36th Annual Logging Symposium, no. 1995-NNN*, Paris, France, 1995.
- [48] Y. Guan, Q. Guo, R. Pu, X. Gao, S. Chen, and T. Ji, "Distribution of Upper Paleozoic coal seams in the Southeastern Ordos basin," *Energies*, vol. 15, no. 14, p. 5110, 2022.
- [49] L. D. Meckel and M. R. Thomasson, "Pervasive tight-gas sandstone reservoirs: an overview," *Vail Hedberg Conference: AAPG Hedberg Series*, vol. 3, pp. 13–27, 2005.
- [50] F. Zhang, J. Liu, and C. Yuan, "Monte Carlo simulation for determining gas saturation using three-detector pulsed neutron logging technology in tight gas reservoir and its application," *Applied Radiation and Isotopes*, vol. 78, pp. 51–56, 2013.